

Simulating Formaldehyde Production and Fluvial Transport on Early Mars using a Global Climate and River Model

*A. Kamada¹, S. Koyama², Y. Furukawa³, T. Kuroda², T. Yoshida², T. Kodama¹, Y. Nakamura⁴, Y. Kasaba², and N. Terada², ¹*Earth-Life Science Institute, Institute of Science Tokyo, Tokyo, Japan (arihiro.kamada@elsi.jp)*, ²*Department of Geophysics, Graduate School of Science, Tohoku University, Sendai, Japan*, ³*Department of Earth Science, Graduate School of Science, Tohoku University, Sendai, Japan*, ⁴*Graduate School of Science, the University of Tokyo, Tokyo, Japan*.

Introduction:

Mars today is a cold and arid planet with a thin atmosphere and a surface pressure of approximately 6.1 mbar and a temperature near 215 K. However, geomorphological and geochemical evidence suggests that early Mars, during the late Noachian to early Hesperian period (approximately 3.8-3.6 Ga), had a markedly different environment; atmospheric pressures likely exceeding 1-2 bar [1] and surface temperatures above the freezing point of water, liquid water was likely stable across broad regions. This epoch is associated with widespread valley networks [2-4], lacustrine deposits [5,6], potentially global oceans [7,8], groundwater activity [9-11], and subsurface phyllosilicate formation [12], all of which are indicative of an active hydrological cycle in the past.

Numerous studies have explored the climatic mechanisms that enabled the stable presence of liquid water on the surface, particularly under dense CO₂ and H₂-rich atmospheres [13-15]. However, comparatively less attention has been given to the chemical environments that may have fostered the emergence of the building blocks of life. Recent photochemical modeling [16] demonstrated that abundant formaldehyde (H₂CO) could have formed on early Mars through UV-driven and redox reactions in a warm, H₂-enriched CO₂ atmosphere. Once produced, H₂CO may have dissolved into rain droplets and been delivered to the surface, where it could have undergone formose reaction to produce complex sugars, including ribose, which is a key building block of RNA.

This raises a fundamental question: Did early Mars have environments that were not only wet and warm, but also chemically enriched enough to support the synthesis, transport, and deposition of organic molecules? In-situ analysis by NASA's Curiosity rover provides critical context. Curiosity detected a substantial inventory of organic carbon within the sedimentary rocks of Gale Crater, which are interpreted as ancient lacustrine mudstones [17]. This finding strongly supports the hypothesis that early Mars had habitable aqueous environments that could concentrate and preserve organic matter.

This study aims to quantify the atmospheric production, deposition by rainfall or snowfall, and subsequent transport of prebiotic organic compounds, particularly H₂CO via fluvial systems to downstream lakes and oceans, under warm early Martian climate condition.

Method:

In this study, we investigated the climate, hydrological, and organic chemical processes of early Mars using a coupled global climate (PMGCM : Paleo-Mars Global Climate Model) [13] and river transport model (CRIS : Catchment-based RIVER Simulator) [14], which simulate global water and material cycle including precipitation, deposition, runoff, and sediment/solute transport on early Mars.

We assumed a CO₂ and H₂O mixing atmosphere with a surface pressure of 2 bar. To create a warm and wet early Mars condition, H₂ mixing ratio of 6% was included, consistent with previous studies suggesting that collision-induced absorption (CIA) between CO₂ and H₂ molecules could significantly warm the planet. We adopted a solar luminosity of ~441 W/m² (approximately 75% of current value for Mars), which corresponds to the reduced luminosity at 3.8 Ga, as modeled by standard solar evolution models [18]. The model used pre-true polar wander (TPW) topography [19], and the elevation below -2.3 km were assumed to be oceans or lakes.

To evaluate H₂CO production, we constructed a lookup table derived from offline 1D photochemical simulations [20], parameterized as a function of temperature, water vapor column, surface pressure, and UV flux. PMGCM provided these atmospheric parameters at each grid point and time step, allowing spatio-temporal estimation of H₂CO production. We estimated H₂CO deposition using Henry's Law, assuming dissolution into rain droplets or adsorption onto snowflakes. CRIS simulated surface runoff, river flow, and sediment/solute transport. This enabled the tracking of the delivery of organic matter from land to terminal basins or the ocean.

Results:

Fig 1 shows annual averaged atmospheric conditions. The temperature structure consists of a warm ocean and cool land surfaces, with a global mean temperature of approximately 292.4 K. Water vapor column density was increased near warm shorelines and oceans due to enhanced evaporation, while inland and polar regions were considerably drier. The UV flux, a key driver of photochemical reactions, also displayed latitudinal variation, being roughly 50% stronger at low latitudes compared to high latitudes. These two variables, water vapor column and UV flux, governed the spatial distribution of atmospheric H₂CO

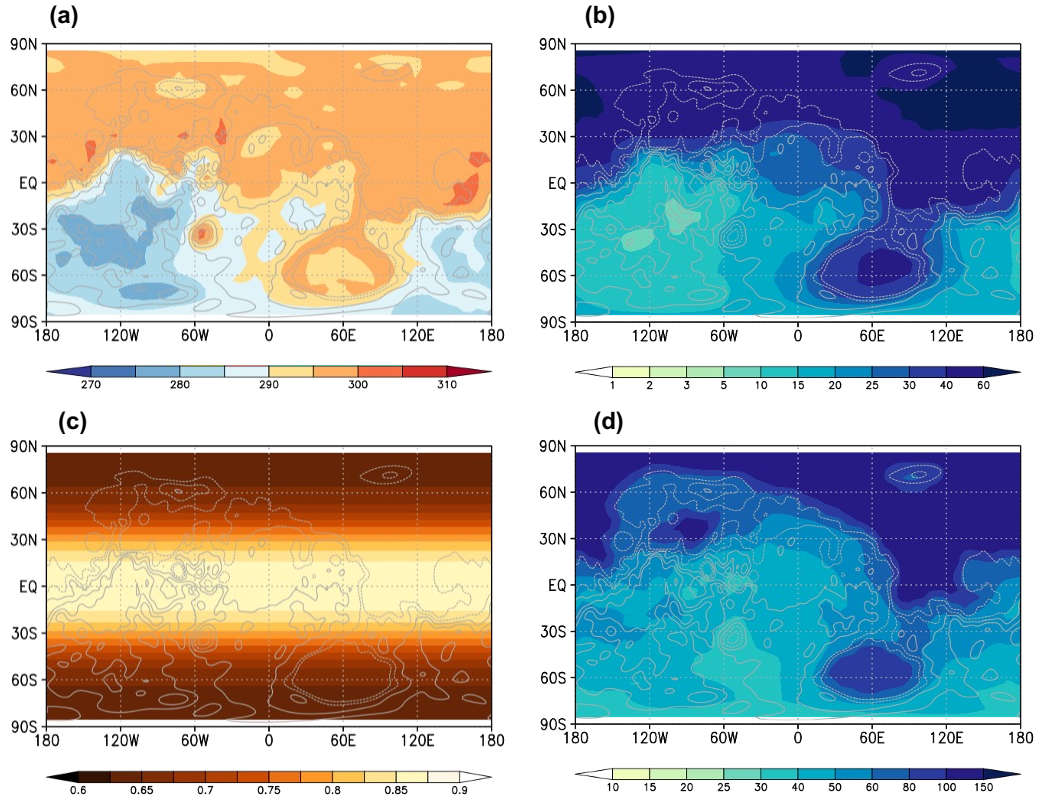


Fig 1. (a) Annual averaged surface temperature [K], (b) water vapor column [$\times 10^{-3}$ kg/m²], (c) TOA UV flux [W/m²], and (d) H₂CO mixing ratio [$\times 10^{-12}$ kg/kg] diagnosed from lookup table.

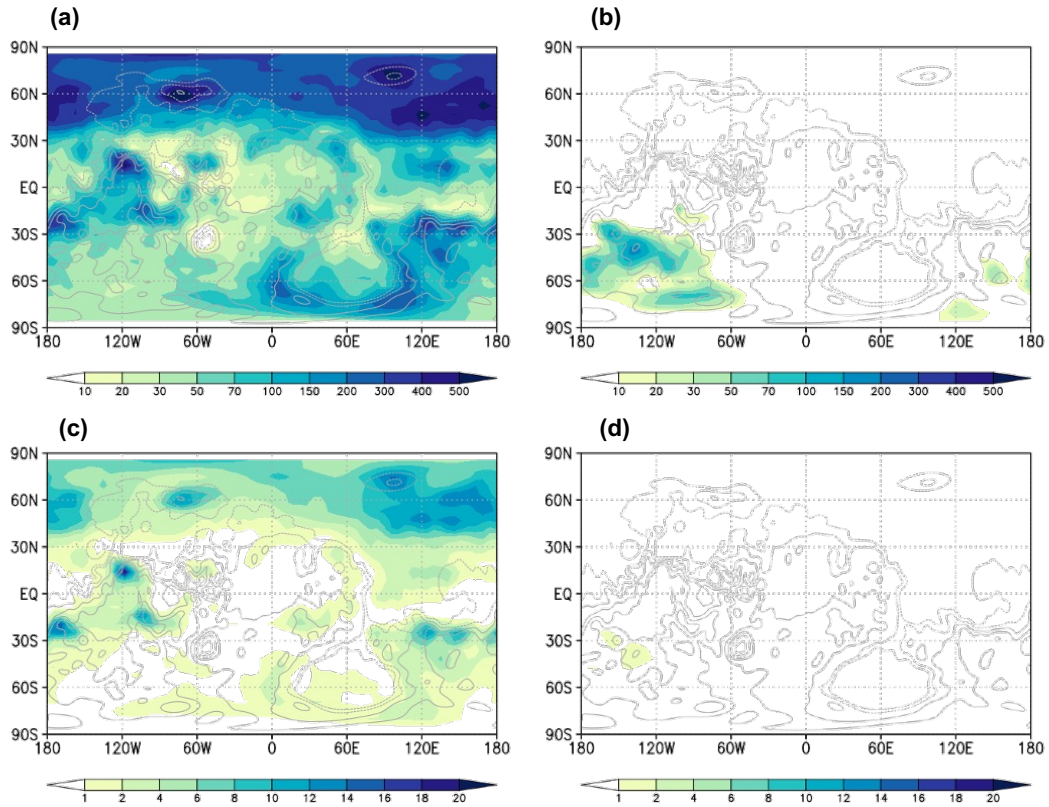


Fig 2. (a) Annual rainfall [mm/yr], (b) snowfall [mm/yr], (c) H₂CO deposition by rainfall [mg/m²/yr], and (d) H₂CO deposition by snowfall [mg/m²/yr].

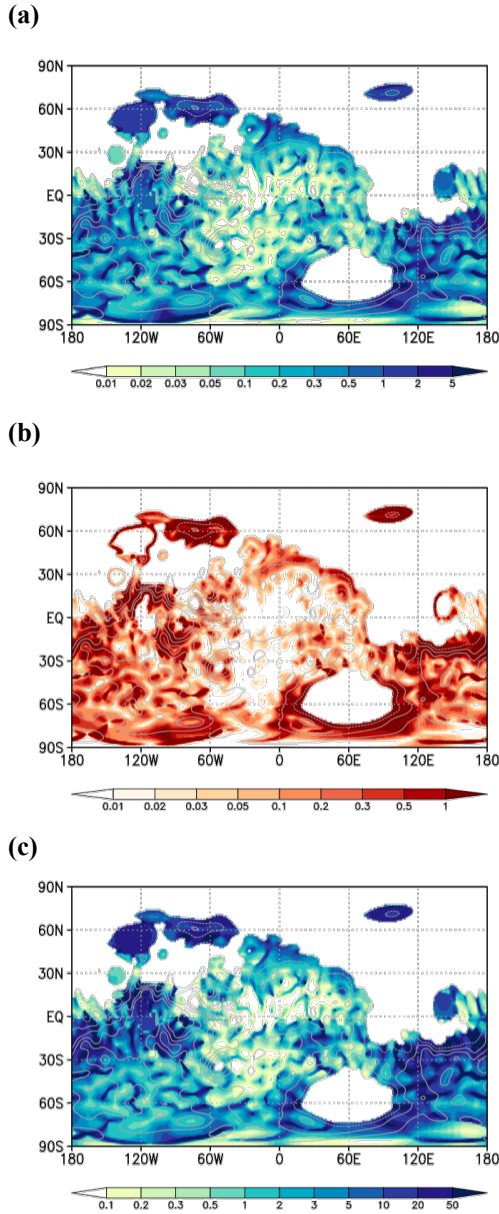


Fig 3. (a) Annual fluvial transport per catchment area [m/year], (b) bedload sediment transport [m/year], and (c) H_2CO transport [$\times 10^{-9}$ m/year].

production. Using precomputed look-up tables, H_2CO production rates were found to be highest in equatorial coastal regions where both moisture and UV levels peaked. In contrast, high-latitude land regions with reduced water vapor column and UV flux exhibited notably lower H_2CO production.

The average annual precipitation on Mars was approximately 119.3 mm per Mars year, consisting of 115.1 mm of rainfall and 4.2 mm of snowfall (see Fig.2). This total is about 10% of Earth's mean annual precipitation. This difference is due to early Martian low solar constant (441 W/m^2), which limited surface evaporation. Rainfall was more prevalent in warmer regions ($T > 273 \text{ K}$), while snowfall was more prevalent in colder continental interiors. The amount of H_2CO deposition depends not only on the amount of

precipitation, but also on the spatial distribution of H_2CO , which is determined by the UV flux and the water vapor column density. The annual surface deposition of H_2CO was $3.8 \times 10^8 \text{ kg}$ for rain droplets and $6.4 \times 10^4 \text{ kg}$ for snowflakes due to the different dissolution/adsorption efficiencies and relatively warm surface condition.

These precipitation and deposition patterns contributed to a dynamic surface fluvial system. Simulated rivers transported water and solutes into terminal basins such as the northern ocean and Hellas basin. Fig.3 showed that large rivers discharged several meters of water per Mars year per unit catchment area, which is comparable to the Amazon River. Sediment transport was likewise significant, estimated at $\sim 0.1\%$ of river flow by volume. Annual sediment transport was calculated to be $4.50 \times 10^8 \text{ m}^3$ to the northern ocean and $0.76 \times 10^8 \text{ m}^3$ to Hellas basin. Transport of organic molecules followed similar patterns. H_2CO , once deposited onto the surface, was partially entrained into river flows. Annually, $\sim 8.53 \times 10^7 \text{ kg}$ of H_2CO was transported to the northern ocean and $\sim 0.20 \times 10^7 \text{ kg}$ to Hellas Basin. These environments may have promoted the formation of complex organic compounds of H_2CO origin in ocean and lakes.

References:

- [1] Kite, E. S., Williams, J. -P., Lucas, A., Aharonson, O., (2014), Low palaeopressure of the Martian atmosphere estimated from the size distribution of ancient craters, *Nat. Geosci.*, 7, 335-339.
- [2] Craddock, R. A. and Howard, A. D., (2002), The case for rainfall on a warm, wet early Mars, *J. Geophys. Res. Planets*, 107(E11), 5111.
- [3] Hynek, B. M., Beach, M., and Hoke, M. R. T., (2010), Updated global map of Martian valley networks and implications for climate and hydrologic processes, *J. Geophys. Res. Planets*, 115(E9).
- [4] Steckel, A. V. et al. (2025), Landscape Evolution Models of Incision on Mars: Implications for the Ancient Climate, *J. Geophys. Res. Planets*, 130, e2024JE008637.
- [5] Grotzinger, J. P. et al. (2014), A Habitable Fluvio-Lacustrine Environment at Yellowknife Bay, Gale Crater, Mars, *Science*, 343, 6169.
- [6] Grotzinger, J. P. et al. (2015), Deposition, exhumation, and paleoclimate of an ancient lake deposit, Gale crater, Mars, *Science*, 350, 6257.
- [7] Di Achille, G. and Hynek, B. M. (2010), Ancient ocean on Mars supported by global distribution of deltas and valleys, *Nat. Geosci.*, 3, 459-463.
- [8] Citron, R. I., Manga, M. and Hemingway, D. J. (2018), Timing of oceans on Mars from shoreline deformation, *Nature*, 555 643-646.
- [9] Andrews-Hanna, J. C., and R. J. Phillips (2007), Hydrological modeling of outflow channels and chaos regions, *J. Geophys. Res.*, 112, E08001.
- [10] Fassett, C. I. and Head J. W. (2008), Valley network-fed, open-basin lakes on Mars: Distribution and implications for Noachian surface and subsurface

hydrology, *Icarus*, 198, 37-56.

[11] Hiatt, E. et al. (2024), Limited recharge of the southern highlands aquifer on early Mars, *Icarus*, 408, 115774.

[12] Bishop, J. L. et al. (2018), Surface clay formation during short-term warmer and wetter conditions on a largely cold ancient Mars, *Nat. Astron.*,

[13] Kamada, A. et al. (2020), A coupled atmosphere-hydrosphere global climate model of early Mars: a 'cool and wet' scenario for the formation of water channel, *Icarus*, 338, 113567.

[14] Kamada, A. et al. (2021), Global climate and river transport simulations of early Mars around the Noachian and Hesperian boundary, *Icarus*, 368, 114618.

[15] Steakley, K. E. et al. (2023), Impact induced H₂-rich climates on early Mars explored with a global climate model, *Icarus*, 394, 115401.

[16] Koyama S. et al. (2024), Atmospheric formaldehyde production on early Mars leading to a potential formation of bio-important molecules, *Scientific Reports*, 14.

[17] Stern, J. C. et al. (2022), Organic carbon concentrations in 3.5-billion-year-old lacustrine mudstones of Mars, *PNAS*, 119(27), e2201139119.

[18] Gough, D. O. (1981), Solar interior structure and luminosity variations, *Sol. Phys.*, 74, 21-34.

[19] Bouley, S. et al. (2016), Late Tharsis formation and implications for early Mars, *Nature*, 531, 344-347.

[20] Nakamura, Y. et al. (2023), Photochemical and radiation transport model for extensive use (PROTEUS), *Earth, Planets and Space*, 75, 140.